

the surface of these samples shows changes that can be seen even with the naked eye. From these figs. we can conclude that corrosion attacks the grain boundaries and this attack can be seen in the presence of white and grows grain boundaries along with red

Table 4 — Unit cell parameters, the crystallite size and the dislocation density of the OL52 and OL52.4 steels before and after corrosion in sea waters

Sample	Corrosion media	A nm	Average crystallite size d, nm	Dislocation density $\delta \cdot 10^{-3}, \text{nm}^{-2}$
OL52	Before corr.	0.2868	15.77	4.02
	Mediterranean Sea	0.2872	17.20	3.38
	Black Sea	0.2870	16.79	3.55
	Aegean Sea	0.2871	19.49	2.63
OL52.4	Before corr	0.2870	15.54	4.13
	Mediterranean sea	0.2871	19.31	2.63
	Black sea	0.2872	18.19	3.02
	Aegean sea	0.2871	17.38	3.31

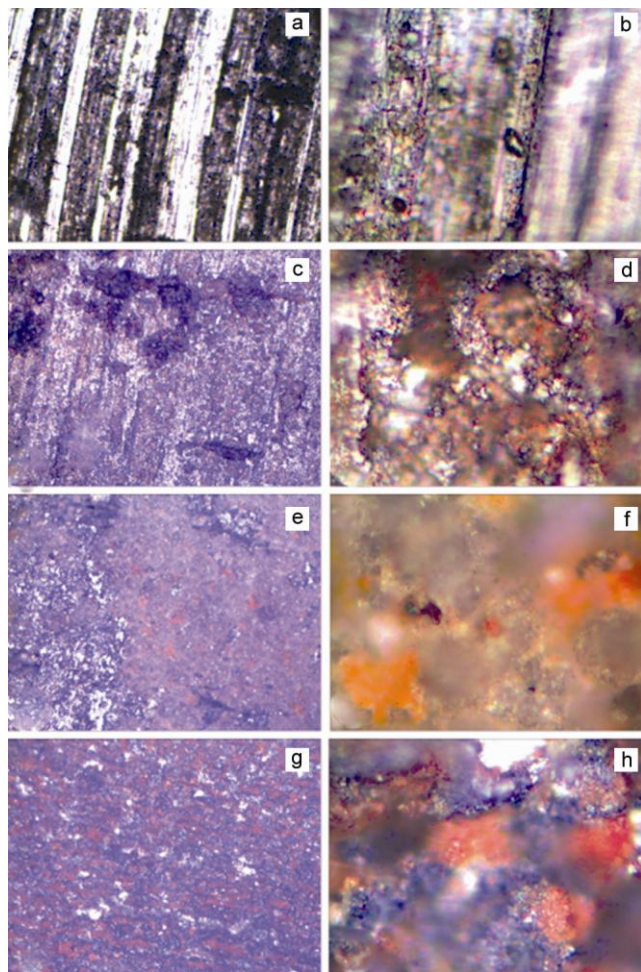


Fig. 5 — Micrographic images of OL 52 with 100× and 800× magnifiers for: a,b) initial state and corroded state: c,d-Black Sea; e,f-Aegean Sea and g,h-Mediterranean Sea

rust. The images for corroded OL52.4 show some white parts which can be aluminium oxide formed in salt water. Those microscopic images sustain the Δm results.

Magnetic properties

Figure 7 presents the temperature behaviour of the specific magnetization, σ , for OL52 and OL52.4 before and after corrosion in the three seawaters in study. The inserts show the dependences $\sigma^2=f(T)$, allowing a more accurate determination of the Curie temperatures, T_c . Steels have a similar nature of dependencies, confirming the presence of free iron. This fact is proved by XRD studies of the sample crystal structure and by chemical composition of studied alloys. In initial state before corrosion action at liquid nitrogen temperature the specific magnetization has a value of $200 \text{ A}\cdot\text{m}^2\cdot\text{kg}^{-1}$ for OL52 and $235 \text{ A}\cdot\text{m}^2\cdot\text{kg}^{-1}$ for OL52.4. It should be noted that the dependences $\sigma=f(T)$ of these

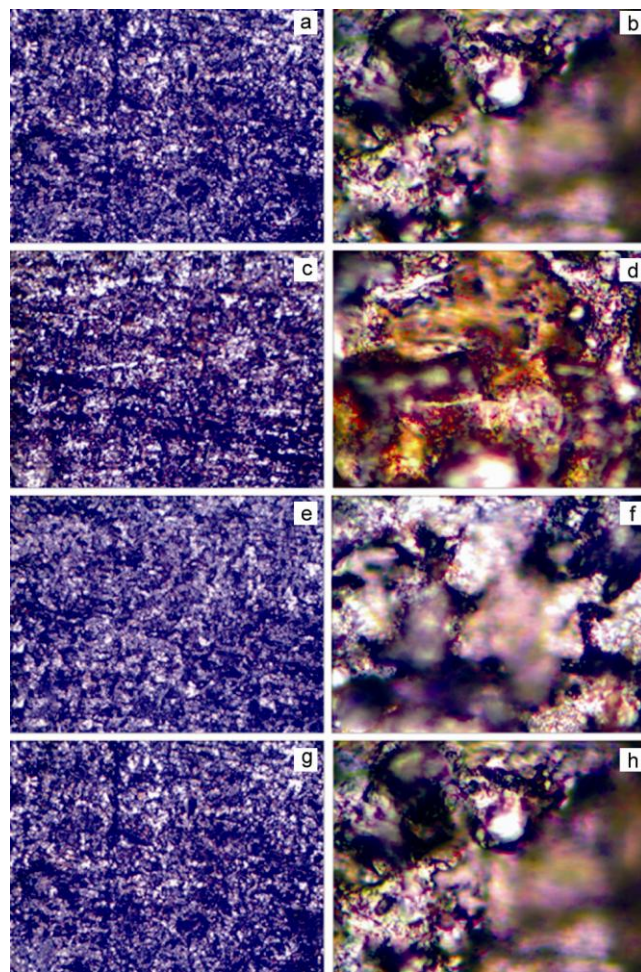


Fig. 6 — Micrographic images of OL 52.4 with 100× and 800× magnifiers for: a,b) initial state and corroded state: c,d-Black Sea; e,f-Aegean Sea and g,h-Mediterranean Sea

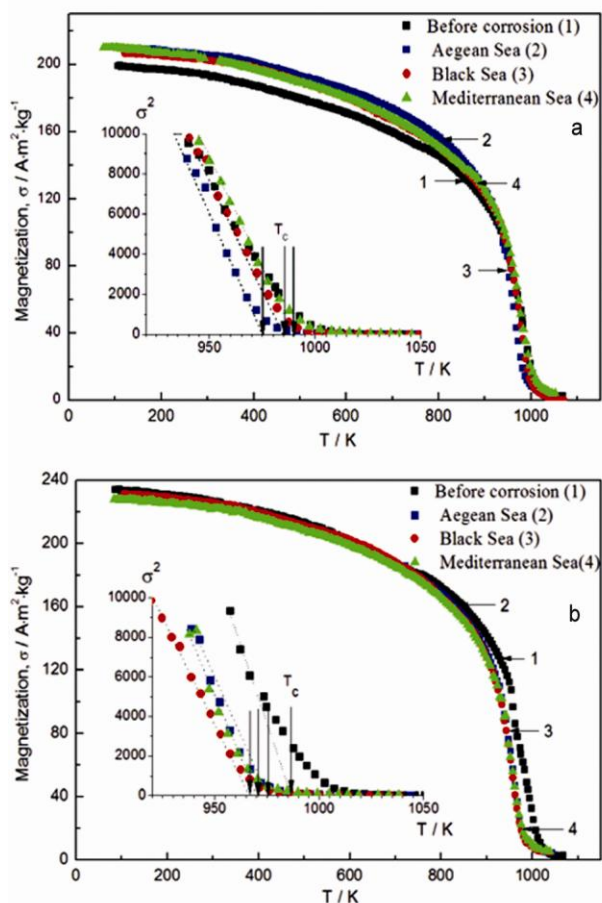


Fig. 7 — Temperature behaviour of specific magnetization for a) OL52 and b) OL52.4

Table 5 — Magnetic parameters of OL52 and OL52.4 alloys before and after the corrosive effects of sea waters

Sample	Corrosion media	T_c K	Σ A·m ² ·kg ⁻¹
OL52	before corrosion	990	203.1
	Mediterranean Sea	990	210.2
	Black Sea	985	206.7
	Aegean Sea	975	209.7
OL52.4	before corrosion	985	233.9
	Mediterranean Sea	970	227.9
	Black Sea	965	231.6
	Aegean Sea	970	228.3

two samples on cooling coincide with the dependences $\sigma=f(T)$ on heating. T_c determined from the dependences $\sigma^2=f(T)$ are 970 K for OL52 and 975 K for OL52.4. A comparative analysis of the specific magnetization temperature dependences and data of Table 5 before and after corrosion action of three sea waters types on OL52 and OL52.4 one can conclude the high corrosion resistance of the stainless steels magnetic characteristics.

The results of such a study can be useful for technologists and designers of constructions based on multifunctional alloys OL52 and OL52.4 in the case of their use in contact with seawaters of various salinity (for example, in the chemical, oil and shipbuilding industries). None of the data in this study could be compared with other data in the literature because this study is the first of its kind on these materials.

Conclusion

1. Weight loss measurements for OL52 and OL52.4 immersed in Aegean, Black and Mediterranean seas show a good corrosion resistance, so these steels can be used in constructions on or near the seawaters.

2. Values of corrosion penetration rate were found to be low (0.047-0.0638 mm·year⁻¹) and microscopic and XRD data sustain these results.

3. At room temperatures in CuK α -radiation the XRD analysis of functional alloys OL52 and OL52.4 samples before corrosion action of sea waters is carried out.

4. Samples of OL52 and OL52.4 alloys have a cubic crystal structure of Im3m sp. gr., with the free iron main phase. The unit cell parameter $a=0.2868$ nm for OL52 steel and $a=0.2870$ nm for OL52.4 steel.

5. The specific magnetization of OL52 and OL52.4 steels in the temperature range of 77-1100 K was studied by ponderomotive method in the 0.86 T magnetic field. It was found that both stainless steels are ferromagnets with a Curie temperature of 970 and 975 K, respectively. At liquid nitrogen temperature, $\sigma=200$ A·m²·kg⁻¹ for OL52 and $\sigma=235$ A·m²·kg⁻¹ for OL52.4. Both stainless steels are resistant to heating up to 1100 K: the temperature dependences $\sigma = f(T)$ are reversible.

Acknowledgement

The work was carried out within the program “Electrode processes, materials for electrochemical processes and corrosion” of the Institute of Physical Chemistry and was supported by the Romanian Academy and the Academy of Sciences of the Republic of Belarus Foundation for Basic Research (project 2018-2019). Authors equally contributed to this work.

References

- 1 Kadhim F S, *Mod Appl Sci*, 5 (2011) 224.
- 2 Knudsen M, *Hydrographical Tables*, (G.E.C. Gad, Copenhagen, Denmark), (1901).

- 3 Subow N N, *Oceanographical Tables*, (Commissariat of agriculture of USSR, Moscow, USSR), (1931).
- 4 Uhlig H H, ed., *Corrosion Handbook*, (Wiley, NY, USA), (1948).
- 5 La Que F L, *Marine Corrosion Causes and Prevention*, (Wiley, NY, USA), (1975).
- 6 Morgan N, *Marine Technology Reference Book*, (Butterworths, London, Boston, UK, USA), (1990).
- 7 Venkatesan R, Venkatasamy M A, Bhaskaran T A, Dwarakadasa E S & Ravindran M, *Br Corros J*, 37 (2002) 257.
- 8 *Sea water corrosion handbook, edited by M M Schumacher*, (Noyes Data Corp, NJ, USA), 1979.
- 9 Ijsseling F P, *Br Corros J*, 24 (1989) 56.
- 10 Orozco-Cruz R, Avila E, Mejia E, Perez T, Contreras A & Martinez R G, *Int J Electrochem Sci*, 12 (2017) 3133.
- 11 Chen X H, Chen C S, Xiao H N, Cheng, F Q, Zhang G & Yi G J, *J Surf Coat Tech*, 191 (2005) 351.
- 12 Ashassi-Sorkhabi H, Ghalebsaz-Jeddi N, Hashemzadeh F & Jahani H J, *Electrochim Acta*, 51 (2006) 3848.
- 13 Jabeera B, Shibli S M A & Anirudhan T S J, *Surf Sci*, 252 (2006) 3520.
- 14 Scherrer P, *Nachr Ges Wiss Gottingen, Math-Phys Kl*, 26 (1918) 98.
- 15 Langford J I & Wilson A J C, *J Appl Cryst*, 11 (1978) 102.
- 16 Popescu A M, Yanuskevich K, Demidenko O, Calderon Moreno J M, Neacsu E I & Constantin V, *Cent Eur J Chem*, 11 (2013) 1137.
- 17 Velaoras D, Zervakis V & Theocharis A, *The physical characteristics and dynamics of the aegean water masses. in: The handbook of environmental chemistry*, (Springer, Berlin, Heidelberg, Germany), (2021).
- 18 El-Etre A Y, *Corr Sci*, 45 (2003) 2485.
- 19 Lebrini M, Bentiss F, Vezin H & Lagrenee M, *Corr Sci*, 48 (2006) 1279.
- 20 El-Naggar M M, *Corr Sci*, 49 (2007) 2226.
- 21 Umoren S A & Ebenso E E, *Matls Chem Phys*, 106 (2007) 387.
- 22 Abd El Rehim S S, Sayyah S M, El-Deed M M, Kamal S M & Azooz R E, *Matls Chem Phys*, 123 (2010) 20.
- 23 Fontana M G, *Corrosion Engineering*, (Tata McGraw-Hill Publishing Company Ltd., New Delhi, India), (2006).
- 27 Ho K H & Roy S K, *Br Corros J*, 29 (1994) 233.
- 28 Roy S K & Ho K H, *Br Corros J*, 29 (1994) 287.
- 29 Heidersbach R H, *Marine Corrosion in Metals Handbook* 9th ed., vol.13, (ASM International, OH, USA), 13 (1987) 893.
- 30 Popescu A M, Soare V, Burada M, Mitrica D, Constantin I, Badilita V, Minculescu F, Cotrut C, Neacsu E I, Donath C & Constantin V, *Indian J Chem Technol*, 25 (2018) 572.
- 31 Castro-Vargas A, Gill S & Paul S, *Surfaces*, 5 (2022) 113.
- 32 Melchers R E, *Corrosion*, 78 (2022) 87.
- 33 Zhang X, Noel-Hermes N, Ferrari G & Hoogeland M, *Corros Mater Degrad*, 3 (2022) 53.
- 34 Li T, Wu J & Frankel G, *Corros Sci*, 182 (2021) 109277.
- 35 Xu Y, Zhou Q, Liu L, Zhang Q, Song S & Huang Y, *Corros Eng Sci Technol*, 55 (2020) 579.
- 36 Googan C, *Marine corrosion and cathodic protection*, (CRC Press-Taylor & Francis Group, Oxfordshire United Kingdom), (2022).